DMD Fast Forward. Published on June 28, 2011 as doi:10.1124/dmd.111.040725

Distribution of KAI-9803, a novel δPKC inhibitor, after intravenous administration to rats

Yoshihiro Miyaji, Sarah Walter, Leon Chen, Atsushi Kurihara, Tomoko Ishizuka, Motoko Saito, Kenji Kawai, and Osamu Okazaki

Drug Metabolism and Pharmacokinetics Research Laboratories, Daiichi Sankyo Co., Ltd., Tokyo, Japan (Y.M., A.K., T.I., M.S., K.K., O.O.)

KAI Pharmaceuticals, South San Francisco, CA, USA (S.W., L.C.)

DMD Fast Forward. Published on June 28, 2011 as DOI: 10.1124/dmd.111.040725
This article has not been copyedited and formatted. The final version may differ from this version.

Running Title:

TAT mediated Distribution of KAI-9803

Address correspondence to:

Yoshihiro Miyaji

Drug Metabolism and Pharmacokinetics Research Laboratories, Daiichi Sankyo Co., Ltd., 1-2-58 Hiromachi, Shinagawa-ku, Tokyo, 140-8710, Japan

Tel: +81-3-3492-3131

Fax: +81-3-5436-8567

E-mail: miyaji.yoshihiro.kc@daiichisankyo.co.jp

Text Pages: 35

Tables: 0

Figures: 8

References: 22

Abstract: 238 words

Introduction: 775 words

Discussion: 1182 words

Abbreviations: HIV-1, Human immune deficiency virus type 1; PKC, protein kinase C; TFA, trifluoroacetic acid; CPP, cell penetrating peptide; PTD, protein transduction domain

Abstract

KAI-9803 is composed of a selective δPKC inhibitor peptide derived from the δV1-1 portion of δPKC (termed "cargo peptide"), conjugated reversibly to the cell penetrating peptide TAT_{47-57} (termed "carrier peptide") via a disulfide bond. KAI-9803 administration at the end of ischemia has been found to reduce cardiac damage caused by ischemia-reperfusion in a rat model of acute myocardial infarction. In the current study, we examined the TAT_{47-57}-mediated distribution of KAI-9803 in rats after a single intravenous bolus administration (1 mg/kg). ^{14}C-KAI-9803 was rapidly delivered to many tissues, including the heart (1.21 μg eq./g tissue), while being cleared quickly from the systemic circulation. The microautoradiography analysis showed that ^{14}C-KAI-9803 was effectively delivered into a variety of cells, including cardiac myocytes and cardiac endothelial cells within 1 minute after dosing. The tissue distribution of ^{125}I-labeled KAI-9803 was compared to that of ^{125}I-labeled cargo peptide, demonstrating that the distribution of KAI-9803 to tissues such as the liver, kidney and heart was facilitated by the reversible conjugation to TAT_{47-57}. In an *in vitro* cardiomyocyte study, the extent of ^{125}I-KAI-9803 internalization was greater at 37˚C than that at 4˚C, while the internalization of the ^{125}I-cargo peptide at 37˚C was not observed, indicating that the uptake of ^{125}I-KAI-9803 into the cardiomyocytes was mediated by the TAT_{47-57} carrier. Our studies demonstrated that after a single intravenous administration, KAI-9803 can be delivered into the target cells in the liver, kidney and heart by a TAT_{47-57}-mediated mechanism.

DMD Fast Forward. Published on June 28, 2011 as DOI: 10.1124/dmd.111.040725
This article has not been copyedited and formatted. The final version may differ from this version.

Introduction

The ability to modulate protein-protein interactions within a cell is a powerful method to control signaling processes and thereby cellular outcomes. Small peptides can interfere with, or potentiate, these protein associations by mimicking core sequences responsible for the interactions, but the delivery of these peptides to the inside of the cell has been a challenge. With the discovery and characterization of cell penetrating peptides (CPPs) or protein transduction domains (PTDs), this hurdle has been largely overcome. One CPP that has been shown to effectively deliver proteins as large as β-glactosidase into cells is the eleven amino acid, arginine-rich sequence of the human immune deficiency virus type 1 (HIV-1) TAT protein (Schwarze et al., 1999; Xia et al., 2001; Cai et al., 2006). Although the exact mechanism by which TAT_{47-57} transports macromolecules into cells is not well defined, evidence suggests the tissue distribution of TAT-fused peptides is partly mediated through interactions with anionic proteoglycans, such as heparan sulfate proteoglycan ubiquitously expressed on the surface of cells. Subsequent to this interaction, TAT-conjugated molecules are believed to enter cells through an energy-dependent process termed macropinocytosis (Tyagi et al., 2001; Console et al., 2003). There are a number of publications demonstrating that TAT can mediate cytosolic delivery of different types of cargo resulting in measurable cytosolic activity (Harada et al., 2002; Tünnemann et al., 2006). Tünnemann et al. reported that TAT-dependent uptake was dependent on the size of the cargo. They show that fusion peptides with cargos of <50 amino acids were rapidly taken up (within 3-5 minutes) and distributed throughout the cell whereas TAT fusion proteins of >50 amino acids were mainly endocytosed and trapped largely in

cytoplasmic vesicles. Therefore, it is believed that short TAT fusion peptides are able to rapidly access the biological target in the cytoplasm in a bioactive manner after internalization.

Upon activation, each PKC isozyme moves, or translocates, to a unique subcellular location where it is anchored via interactions with its isozyme-specific receptor for activated C kinase (RACK). It is the interaction with the isozyme-specific RACK that determines the functional specificity of the isozyme by bringing PKC in contact with its substrates (Mochly-Rosen, 1995; Mochly-Rosen and Gordan, 1998). Recently, peptides derived from PKC have been described which can be delivered into cells by CPPs and thus disrupt the critical protein-protein interactions responsible for isozyme-specific PKC translocation and consequent activity. When such PKC-modulating peptides are reversibly conjugated to the CPP by a disulfide bond, the "cargo" peptides can be released from the "carrier" peptides by cleavage of the disulfide bond once inside the reducing environment of the cell (Chen et al., 2001b). One PKC modulating peptide currently in clinical development is KAI-9803. KAI-9803 is composed of a selective δPKC inhibitor peptide (termed "cargo peptide") formed from the δV1-1 region of δPKC (Chen et al., 2001a), conjugated reversibly to the TAT_{47-57} carrier peptide by a disulfide bond. KAI-9803 was found to selectively inhibit δPKC translocation and reduce cardiac damage in cardiomyocytes, caused by ischemia-reperfusion both in *ex vivo* models and in *in vivo* models of cardiac disease (Chen et al, 2001a, 2001b; Inagaki et al., 2003a, 2003b; Ikeno et al., 2007). A single intraperitoneal injection of KAI-9803 in mice also resulted in the selective inhibition of δPKC translocation in the liver, kidney, lung, heart and brain (Begley et al., 2004). KAI-9803 is currently under clinical development for cardioprotection from

DMD Fast Forward. Published on June 28, 2011 as DOI: 10.1124/dmd.111.040725
This article has not been copyedited and formatted. The final version may differ from this version.

ischemia-reperfusion damage in ST-elevation acute myocardial infarction (AMI), and local administration to the coronary artery of ST-elevation AMI patients results in the improvement of key biomarkers of myocardial damage (Bates et al., 2008).

However, there is little information on the tissue distribution and the distribution mechanisms of KAI-9803 after a single intravenous administration. Furthermore, the *in vivo* tissue distribution of small peptides reversibly conjugated to TAT_{47-57} following systemic dosing has not been fully demonstrated, although there are many reports that the permanent covalent attachment of TAT_{47-57} results in enhancement of the distribution of limited kinds of "cargo" large proteins such as β-glucuronidase throughout the body (Schwarze et al., 1999; Xia et al., 2001; Cai et al., 2006). The goal of the present study is to quantitatively determine the tissue distribution of KAI-9803 and to propose a mechanism of tissue uptake following systemic, intravenous administration in rats. We show here that KAI-9803 is taken up into a variety of tissues such as the liver, kidney and heart after an intravenous injection, and is delivered into cardiac myocytes and endothelial cells. Also, we demonstrate the internalization of KAI-9803 into cardiomyocytes *in vitro*. Through comparing distribution patterns of cargo alone vs. intact KAI-9803, we are able to show here that the tissue uptake of KAI-9803 is a TAT_{47-57}-dependent mechanism.

DMD Fast Forward. Published on June 28, 2011 as DOI: 10.1124/dmd.111.040725
This article has not been copyedited and formatted. The final version may differ from this version.

Materials and Methods

Peptide synthesis: δV1-1 cargo and KAI-9803.

We synthesized δV1-1 cargo peptide (composed of amino acids 8 to 17 from δPKC plus a cysteine at the N-terminus [C-SFNSYELGSL]), to be used for disulfide conjugation with TAT_{47-57} [C-YGRKKRRQRRR], to create KAI-9803. [SFNSYELGSL] was synthesized as the δV1-1 cargo peptide to be used as the control peptide in the tissue distribution study.

^{14}C-labeled KAI-9803 (Lot No. CFQ14916) in which only the cargo portion was ^{14}C-labeled, was synthesized by GE-Healthcare UK Ltd. (Little Chalfont, UK). The chemical structure of ^{14}C-KAI-9803 and its ^{14}C-labeled position are shown in Fig. 1. The synthesis was done in the following manner: ^{14}C-labeled cargo peptide was first synthesized using ^{14}C-labeled tyrosine, which was uniformly labeled on the benzene ring carbons. Then ^{14}C-labeled cargo peptide was coupled through a disulfide bond with the TAT_{47-57} peptide. The specific radioactivity was 3.41 MBq/mg (204.38 dpm/mg), and the radiochemical purity of ^{14}C-KAI-9803 was shown to be more than 97% by measurements using reversed phase-HPLC under the conditions described below just before dosing.

Radioiodination of KAI-9803 and cargo peptide.

KAI-9803 (100 μg) and the cargo peptide (25 μg) were labeled with 1 mCi of sodium ^{125}I-iodide (PerkinElmer, Inc, Waltham, MA) using a modified lactoperoxidase method as previously described (Thorell et al., 1971). Sample iodination was performed in 50 μl of 0.3 M acetate buffer (pH5.0, containing 0.01% polysorbate 80)

DMD Fast Forward. Published on June 28, 2011 as DOI: 10.1124/dmd.111.040725
This article has not been copyedited and formatted. The final version may differ from this version.

supplemented with 4 µg lactoperoxidase (Sigma-Aldrich Corp., St. Louis, MO), 1 mCi of ^{125}I-Na and 0.035 µmol of each peptide. The reaction was started by the addition of 10 µl of hydrogen peroxide (0.88 mM), and then hydrogen peroxide was added three more times at 5 minute intervals. The reaction was maintained at room temperature for 20 minutes after the reaction started. The peptide-associated radioactivity was separated from the free ^{125}I-idodine using a MicroSpin G-25 column (GE Healthcare UK Ltd.) equilibrated with 0.3 M acetate buffer (pH 5.0, containing 0.01% polysorbate 80). It was confirmed that the peptides were stable in the reaction system, especially against hydrogen peroxide. The concentration of ^{125}I-labeled peptide stock solution was determined using the DC protein assay kit (Bio-Rad Laboratories, Inc., Hercules, CA) with each of the peptides as a standard. The radioactivity in the samples was determined by γ-irradiation counting for 1 minute using an Auto-Gamma Counting Systems RiaStar (PerkinElmer, Inc.).

Just prior to dosing, the radiochemical purity of each ^{125}I-labeled peptide in each dosing solution was confirmed to be more than 97%, as analyzed by size exclusion chromatography-HPLC analysis, using a Shimadzu LC-10Avp HPLC system (Kyoto, Japan). The effluent was monitored optically at 206 nm, and radiolabeled peptide was detected with an on-line (RI)-detector (Radiomatic 525TR; PerkinElmer, Inc.). The mobile phase was 50 mM acetate buffer (pH 5.0, containing 0.3 M NaCl/0.02% Tween 20)/acetonitrile =80/20 (v/v), at a flow rate of 0.5 mL/min and with a 50 minute assay time. A Superdex peptide 10/300GL column (GE-Healthcare UK Ltd.) was used to identify the purity of the radiolabeled peptide.

Reversed phase (RP)-HPLC conditions for bioanalysis.

DMD Fast Forward. Published on June 28, 2011 as DOI: 10.1124/dmd.111.040725
This article has not been copyedited and formatted. The final version may differ from this version.

The radiochemical purity assay of ^{14}C-labeled KAI-9803 in the dosing solution and the analysis of the metabolite profile of ^{14}C-KAI-9803 in the bile and plasma samples were performed by reversed phase (RP)-HPLC using a Shimadzu LC-10Avp HPLC system with an on-line radioisotope (RI)-detector. The HPLC conditions were as follows: Mobile phase A was water containing 0.1% trifluoroacetic acid (TFA) and mobile phase B was acetonitrile containing 0.1% TFA. Aliquots of the plasma and bile samples and the dosing solution diluted 10-fold with purified water were injected onto a 150 × 4.6 mm, 5 μm TSKgel ODS-80TM column (TOSOH Corporation, Tokyo, Japan) maintained at 25°C. The mobile phase at a flow rate of 1 mL/min was a linear gradient which started at 95% A and 5% B, rose to 40% B over 25 minutes, rose to 90% B over 1 minute from 25 to 26 minutes, maintained at 90% B to 27 minutes, then declined to 5% B over 1 minute from 27 to 28 minutes, and maintained at 5% B to 34 minutes. The eluate from the analytical column was monitored by a UV detector (206 nm) and RI-detector with a 34-minute assay time. Ultima-Flo M (PerkinElmer, Inc.) was used as the scintillation fluid cocktail at a flow rate of 2 mL/minute. In this system, the retention time of KAI-9803 was 20 minutes. The column recovery of ^{14}C-KAI-9803 was more than 96%. The ratio of the peak area of ^{14}C-KAI-9803 to the total peak area over the run time was calculated as the radiochemical purity using Flo-One for Windows (ver. 3.60, PerkinElmer, Inc.).

Animal studies.

Six-week old male Crl:CD(SD) rats were purchased from Charles River Japan, Inc. (Kanagawa, Japan), and acclimatized for one week in a controlled animal area set at a room temperature of 23 ± 2°C and relative humidity of 55 ± 5% under a 12-hour cycle

DMD Fast Forward. Published on June 28, 2011 as DOI: 10.1124/dmd.111.040725
This article has not been copyedited and formatted. The final version may differ from this version.

of light/dark artificial lighting. All rats were allowed *ad libitum* access to food and water. The rats were fasted overnight before the experiments. Tap water was given *ad libitum* throughout the study. Experiments were conducted in accordance with the Institutional Guidelines for the care and Use of Laboratory Animals.

Each of ^{14}C-KAI-9803 and ^{125}I-labeled peptides was dissolved in 4% mannitol solution just before dosing. The dosing solutions were intravenously administered to rats under ether anesthesia (1 mL/kg). For pharmacokinetic studies, ^{14}C-KAI-9803 (1 mg/kg) was administered to rats via the femoral vein and approximately 0.2 mL of blood was collected from the jugular vein at 1, 2, 5, 10 and 15 minutes post-dose with a heparinized syringe containing 10 μL of 400 mM diisopropylfluorophosphate dissolved in acetonitrile to prevent rapid degradation of the peptide. The radioactivity in the blood and plasma samples was measured using a liquid scintillation counter. The nanogram equivalent of ^{14}C-KAI-9803 in the plasma and blood was calculated by dividing the radioactivity (dpm/mL) of the measurement sample by the specific radioactivity of ^{14}C-KAI-9803 (204.38 dpm/ng) and the plasma and blood radioactivity concentrations are expressed as a unit of ng eq./mL. For analysis of the *in vivo* metabolite profile in the plasma, ^{14}C-KAI-9803 (10 mg/kg) was injected to rats and approximately 0.1 mL of blood was collected with a syringe which contained 0.1 mL of 0.263 M citrate buffer (pH 2.0, containing 24 mg/10 mL of K_2EDTA) to prevent the degradation of ^{14}C-KAI-9803. The plasma sample was analyzed by RP-HPLC. The plasma samples were stored in ice until the HPLC analysis.

For determination of biliary and urinary excretion of the radioactivity, ^{14}C-KAI-9803 (1 mg/kg) was administered to bile-duct cannulated rats via the tail vein. After dosing, the rats were kept in Bollman cages (Sugiyama Gen Iriki Co., Ltd., Tokyo,

DMD Fast Forward. Published on June 28, 2011 as DOI: 10.1124/dmd.111.040725
This article has not been copyedited and formatted. The final version may differ from this version.

Japan) to collect bile and urine. Bile and urine were collected for 48 hours post-dose at 4°C. All the bile and urine samples were counted in a liquid scintillation counter and were analyzed by RP-HPLC.

Measurement of radioactivity in dosing solution and biological samples by liquid scintillation counting.

The radioactivity in the dosing solution and the samples were determined by liquid scintillation counting using a 2300TR counter (PerkinElmer, Inc.). Each aliquot was then weighed and mixed with 1 mL of a tissue solubilizer, NCS-II (GE Healthcare UK Ltd.) and 10 mL of liquid scintillator, Hionic-Fluor (PerkinElmer, Inc.). The blood samples were decolorized with 30% hydrogen peroxide before counting. The tissue samples obtained in the whole-body autoradioluminography were decolorized with 30% hydrogen peroxide, solubilized with 1 mL of NCS-II at 50°C overnight, and then added to 10 mL of Hionic-Fluor. The counting efficiency was corrected by the external standard source method.

Whole-body autoradioluminography and Imaging analysis.

Whole-body autoradioluminography was conducted. After administration of ^{14}C-KAI-9803 (1 mg/kg) to rats via the tail vein, the rats were euthanized with CO_2 at 1, 5, 30 and 60 minutes post-dose, then fixed by flash-freezing in an n-hexane/dry ice bath and embedded in 5% carboxymethyl cellulose. Fifty-μm thick sagittal cryosections were prepared using Cryomicrotome (CryoMacrocut CM-3600, Leica Microsystems Nussloch GmbH, Wetzlar, Germany). The sections were exposed to an imaging plate (BAS-III, Fuji Photo Film Co., Ltd., Tokyo, Japan) for 24 hours. The imaging plates

were then subjected to an imaging analysis using a Bio Imaging Analyzer (FUJIX BAS-2500, Fuji Photo Film Co., Ltd.). The relative intensity of the radioactivity was determined for each tissue and the obtained value was expressed as the Photo-Stimulated Luminescence (PSL) per unit area (mm^2). For quantification of the tissue concentration of ^{14}C-KAI-9803, the brain, liver, blood, testes and thymus were collected from the residual cellulose block that had been generated from rats at 1, 5, 30 and 60 minutes post-dose. The radioactivity concentrations (dpm/g) in the isolated tissues were measured using a liquid scintillation counter. The radioactivity concentration in each tissue (dpm/g) was plotted against the PSL/area value in the corresponding tissue to obtain a calibration curve. The PSL/area values in other tissues were converted to the radioactivity concentrations (dpm/g) using the calibration curve. The microgram equivalent of ^{14}C-KAI-9803 in the tissue was calculated by dividing the tissue radioactivity concentration (dpm/g) by the specific radioactivity of ^{14}C-KAI-9803 (204.38 dpm/ng), and was expressed as a unit of μg eq./g tissue. One rat was used per time point.

Microautoradiography.

After administration of ^{14}C-KAI-9803 (1 mg/kg) to the rat via tail vein, the rat was decapitated at 1 minute post-dose and exsanguinated and the liver, kidneys, lungs, heart and brain were immediately excised to prepare microautoradiograms. Each block (about 7 × 7 mm^2) of each excised tissue was embedded with OCT compound (Tissue-Tek, Sakura Finetek Japan Co., Ltd., Tokyo, Japan) in a prepared aluminum mold and frozen in liquid propane. Five-μm thick cryosections were prepared using Cryostat (Leica CM-3000, Leica Microsystems Nussloch GmbH), and the sections were

DMD Fast Forward. Published on June 28, 2011 as DOI: 10.1124/dmd.111.040725
This article has not been copyedited and formatted. The final version may differ from this version.

mounted on glass slides pre-coated with nuclear emulsion (LM-1, GE-Healthcare UK Ltd.) and dried. The mounted sections were placed in a dark box at 4°C for at least 4 days. After exposure, the sections were developed, stained with hematoxylin-eosin, dried at room temperature and enclosed with Entellan new mounting medium (Merck KGaA, Darmstadt, Germany) for microscopic observation. The distribution of radioactivity was confirmed by black grain (bright field) or white grain (dark field) derived from the exposed silver grain.

Tissue distribution of ^{125}I-KAI-9803 and ^{125}I-cargo peptide after intravenous administration.

^{125}I-KAI-9803 (0.35 μmol/kg) was intravenously administered to rats (n = 4-5) via the left femoral vein 1 minute after the intravenous administration of heparin (180 USP units/mg, Sigma-Aldrich Co.) dissolved in 4% mannitol (1 mg/kg or 100 mg/kg), via the right jugular vein. Heparin was used as a competitive inhibitor for the binding of TAT_{47-57} to cell surface heparan sulfate proteoglycans (Kaplan et al, 2005). In a separate, control arm of the study, ^{125}I-KAI-9803 or ^{125}I-cargo peptide was intravenously administered to rats (n = 4-5) 1 minute after intravenous dosing of a 4% mannitol solution (1 ml/kg). One minute after the administration of each of the ^{125}I-labeled peptides, blood was taken via the abdominal aorta with a heparinized syringe and the rats were sacrificed. Then the liver, kidneys, spleen, lungs and heart were removed, rinsed with saline, and weighed. The radioactivity in the blood and tissue samples was determined by γ-irradiation counting for 1 minute. The radioactivity in each tissue was expressed as a percentage injected dose per gram tissue (% of dose /g).

DMD Fast Forward. Published on June 28, 2011 as DOI: 10.1124/dmd.111.040725
This article has not been copyedited and formatted. The final version may differ from this version.

Cells and cell culture.

Neonatal cardiomyocytes from 2- to 3-day-old male Crl:CD(SD) rats, were purchased from Primary Cell Co., Ltd. (Hokkaido, Japan). The rat cardiomyocytes were isolated with collagenase as described earlier (Yuki et al., 2000) with slight modifications. The cells were suspended in DMEM/F-12 (Gibco BRL, Rockville, MD) supplemented with 10% heat-inactivated fetal bovine serum, 100 U/mL penicillin and 100 μg/mL streptomycin. The cells were cultured in tissue culture flasks for 1 hour at 37˚C to separate the myocytes from the noncardiomyocytes. The unattached myocyte suspension was then collected and pelleted by centrifugation. The myocytes were resuspended in DMEM/F-12 containing 10% fetal bovine serum and ITS-X supplement (Invitrogen Corporation, Carlsbad, CA), and were plated in a collagen-coated 24-well plate at a density of 0.5×10^5 cells/cm^2. The cells were incubated in a humidified atmosphere containing 5% CO_2 at 37˚C overnight. Before starting the experiments, the cells were washed three times with 0.5 mL/well of the assay medium (serum-free DMEM/F-12 containing 100 U/mL penicillin and 100 μg/mL streptomycin), and pre-incubated in 0.5 mL/well of the assay medium for 20 minutes at 37˚C or 4˚C prior to any further additions.

Determination of Internalization.

Internalization of ^{125}I-KAI-9803 or ^{125}I-cargo peptide into myocytes was determined at 37˚C or at 4 ˚C. The assay was performed in 0.5 mL/well of the assay medium containing ^{125}I-KAI-9803 (10 nM) or ^{125}I-cargo peptide (10 nM). At designated times, the medium was collected and the cells were washed twice with 0.5

DMD Fast Forward. Published on June 28, 2011 as DOI: 10.1124/dmd.111.040725
This article has not been copyedited and formatted. The final version may differ from this version.

mL/well of ice-cold PBS (pH 7.4). Each well then received 0.5 mL of ice-cold 1 mg/mL heparin solution containing 2 M NaCl and was incubated for 10 minutes at 4˚C to remove the cell-surface bound radioactivity. Heparin eluate from the cells was collected. The cells were solubilized in 1 mL/well of 1 N NaOH for 30 minutes. The radioactivity of each ^{125}I-peptide in the incubation medium, and the cell lysate was determined by γ-irradiation counting. The degree of internalization of each ^{125}I-peptide was expressed as a ratio of the counts in the cell lysate, divided by the total micrograms of cellular protein to the counts in the medium per μl of liquid. After neutralizing the cell lysate, the cellular protein content was determined using a DC protein assay kit with bovine serum albumin as a standard. The heparin-wash removed more than 90% of the cell-associated radioactivity obtained by 4˚C incubation. All measurements were performed in duplicate in three independent experiments.

Statistical Analysis.

All data were expressed as the mean±S.D. or S.E. of more than three experiments. The tissue distribution per gram tissue (% of dose/g tissue) for each of the ^{125}I-cargo peptide and ^{125}I-KAI-9803 with added heparin was compared with that for ^{125}I-KAI-9803 alone by a Dunnett's test. The statistical analysis was performed by using the SAS System version 8.2 (SAS Institute Inc., Cary, NC). Differences were considered to be significant when $p < 0.05$.

DMD Fast Forward. Published on June 28, 2011 as DOI: 10.1124/dmd.111.040725
This article has not been copyedited and formatted. The final version may differ from this version.

Results

Blood and plasma concentrations of radioactivity and plasma metabolite profiles after intravenous administration of ^{14}C-KAI-9803.

The blood and plasma radioactivity levels were determined after intravenous administration of ^{14}C-KAI-9803 at a dose of 1 mg/kg (Fig. 2). The blood/plasma radioactivity ratio ranged from 0.627 - 0.808, suggesting that the blood cell distribution of ^{14}C-KAI-9803 was minimal. The total radioactivity was eliminated from the blood and plasma with calculated half-lives of 9.67 and 8.18 minutes, respectively. As these half-lives are a measure of total radioactivity present, the signals most likely reflect the presence of radiolabeled degradation products/metabolites of KAI-9803.

Rats were administered ^{14}C-KAI-9803 at a dose of 10 mg/kg, and the metabolite profiles in plasma at 1, 2 and 5 minutes post-dose were analyzed by RP-HPLC. Typical HPLC chromatograms of plasma samples at 1 and 5 minutes post-dose and that of the dosing solution are shown in Fig. 3A. The disappearance of the intact compound over time was calculated from the chromatograms and is shown graphically in Fig. 3B. The chromatogram of the dosing solution showed a clear single peak at a retention time of 20 minutes. A significant portion of the radioactivity was observed at a retention time of 20 minutes on the chromatogram of the plasma at 1 minute post-dose, and there were minimal degraded products of ^{14}C-KAI-9803, suggesting that the unchanged form of ^{14}C-KAI-9803 accounted for almost all the ^{14}C radioactivity present in the plasma at 1 minute post-dose. The largest radioactivity peak on the chromatogram of plasma at 5 minutes post-dose was observed at a retention time of approximately 7 minutes, which is coincident with that of tyrosine, suggesting

rapid metabolism of ^{14}C-KAI-9803 had occurred by five minutes (Fig. 3A). The parent compound was rapidly eliminated from the circulation with a half-life of 1.58 minutes (Fig. 3B).

Biliary and urinary excretion ratio of radioactivity after intravenous administration of ^{14}C-KAI-9803 to rats.

The biliary and urinary routes of elimination were then examined as possible explanations for the rapid clearance of KAI-9803 from the bloodstream. The cumulative biliary and urinary excretion of the radioactivity was determined after intravenous administration of ^{14}C-KAI-9803, and is shown in Fig. 4. At 48 hours post-dose, the cumulative biliary and urinary excretion ratios of the radioactivity were 5.75% and 2.99% of the given dose, respectively. The RP-HPLC metabolite profile of ^{14}C-KAI-9803 demonstrated that there was no intact ^{14}C-KAI-9803 present at 1 hour post dose in the bile or in any of the urine samples, but one peak identical with that of tyrosine only (data not shown). These results indicate that ^{14}C-KAI-9803 was minimally, if at all, excreted to the bile and urine in intact or metabolized form.

Tissue distribution of ^{14}C-KAI-9803 by quantitative whole-body autoradioluminography.

Tissue distribution after intravenous administration of ^{14}C-KAI-9803 (1 mg/kg) was quantitatively evaluated by whole-body autoradioluminography. The representative section at 1 minute post-dose is shown in Fig. 5A. At 1 minute post-dose a majority of the radioactivity in the plasma is present as the intact form of ^{14}C-KAI-9803 (Fig. 3), thus it is a reasonable assumption that the radioactivity

distribution in tissues at this time point also represents the intact form of the compound. The radioactivity levels were relatively high in well-vascularized organs such as the liver, kidneys, spleen, lungs and heart. A small amount of radioactivity was found in the central nervous system (the brain, spinal cord) and eyes. The tissue concentrations of ^{14}C-KAI-9803 (μg eq./g tissue) were calculated from the whole-body autoradioluminograms and are shown in Fig. 5B. The radioactivity concentrations were relatively high in the liver (2.64 μg eq./g tissue) and the renal cortex (2.98 μg eq./g tissue). The radioactivity concentrations in the lungs, spleen, heart and blood were 1.43, 1.24, 1.21 and 1.95 μg eq./g tissue, respectively. These data demonstrate that ^{14}C-KAI-9803 was delivered to a variety of tissues including the heart, the primary intended target of KAI-9803.

Microautoradiography.

Microautoradiography was used in order to look more specifically at the delivery of ^{14}C-KAI-9803 into cells of various tissues. Fig. 6 shows microautoradiograms of various tissues 1 minute after intravenous administration of 1 mg/kg ^{14}C-KAI-9803. Microautoradiograms of the liver revealed strong labeling with silver grains throughout the liver, and extremely high radioactivity was found around the blood vessels (Fig. 6A and B). These results demonstrate that ^{14}C-KAI-9803 was rapidly delivered into the hepatocytes. No radioactivity was found in the bile duct, suggesting that little radioactivity was excreted to the bile at this acute time point post-dose. The labeling in the kidneys was localized to specific zones. It was concentrated in the epithelial cells in the proximal convoluted tubules but not in the glomeruli (Fig. 6C and D). In the lungs, the labeling was found in the layer of smooth muscle localized around the

DMD Fast Forward. Published on June 28, 2011 as DOI: 10.1124/dmd.111.040725
This article has not been copyedited and formatted. The final version may differ from this version.

bronchioles (Fig. 6E and F). No labeling was found in the terminal bronchioles and alveoli (data not shown). In the heart, high radioactivity was found in the cardiac myocytes and cardiac endothelial cells, as well as in the blood vessels (Fig. 6G and H), indicating that ^{14}C-KAI-9803 was delivered into cardiac myocytes and endothelial cells after intravenous administration. In the brain, a high degree of labeling was found in the blood vessels. Little radioactivity was found in the cerebral cortex and caudate putamen located 0.48 mm anterior from Bregma (Fig. 6I and J), suggesting that ^{14}C-KAI-9803 was not delivered into the cerebral parenchyma through the blood-brain barrier 1 minute after dosing.

TAT$_{47-57}$-mediated tissue distribution.

To determine whether the tissue distribution of KAI-9803 was dependent on TAT$_{47-57}$, the tissue distribution of the intact form of ^{125}I-KAI-9803 was compared with that of ^{125}I-cargo peptide alone at 1 minute after intravenous administration at 0.35 μmol/kg (1 mg/kg of KAI-9803 and 0.4 mg/kg of cargo peptide) (Fig. 7). As it has been shown in multiple publications that TAT$_{47-57}$ acts as a cell penetrating peptide carrier, it was not surprising that the tissue distribution of ^{125}I-cargo peptide, without the TAT$_{47-57,}$ was significantly lower in the liver, kidneys, heart and spleen than that of intact ^{125}I-KAI-9803. To further demonstrate the role that TAT$_{47-57}$ plays in cellular uptake, heparin was used as a competitive inhibitor for the binding of TAT$_{47-57}$ to cell surface heparan sulfate proteoglycans. A high dose of heparin (100 mg/kg) administered just prior to KAI-9803 dosing, significantly decreased the uptake of ^{125}I-KAI-9803 in the liver and heart, while resulting in an increased signal in the kidneys and blood. When this experiment was repeated with a lower dose of heparin

DMD Fast Forward. Published on June 28, 2011 as DOI: 10.1124/dmd.111.040725
This article has not been copyedited and formatted. The final version may differ from this version.

(1 mg/kg = ca.180 USP units/kg), one typically used in clinical situations, no effect was observed on the tissue distribution of ^{125}I-KAI-9803.

Internalization of ^{125}I-KAI-9803 in rat cardiomyocytes.

Internalization of KAI-9803 was examined more closely in cell culture using primary rat cardiomyocytes. Fig. 8 shows a time-course of internalization of ^{125}I-KAI-9803 and ^{125}I-cargo peptides. To determine cellular uptake, cells were incubated with either ^{125}I-cargo peptide or ^{125}I-KAI-9803 and then treated with very high doses of heparin to compete off any cell-surface bound material. As would be expected with a TAT_{47-57}-dependent process, the internalization of ^{125}I-KAI-9803 at 37˚C was much higher than at 4˚C. The internalization of ^{125}I-cargo peptide at 37˚C was minimal and did not increase over time. These results indicated that ^{125}I-KAI-9803 was internalized into the cardiomyocytes in a process dependent upon TAT_{47-57}.

DMD Fast Forward. Published on June 28, 2011 as DOI: 10.1124/dmd.111.040725
This article has not been copyedited and formatted. The final version may differ from this version.

Discussion

KAI-9803 is composed of a δPKC inhibitor peptide derived from the δV1-1 region of δPKC reversibly conjugated to TAT_{47-57} by a disulfide bond. KAI-9803 has been shown to be a therapeutic candidate for ischemia/reperfusion damage in the heart in preclinical and clinical studies (Bates et al., 2008), and is currently in clinical development for cardioprotection from ischemia/reperfusion injury. In the present study we assessed the tissue distribution of ^{14}C-KAI-9803 and its mechanisms after a single intravenous administration to rats. In addition, we assessed the micro-localization of ^{14}C-KAI-9803 in tissues using microautoradiography. The most notable finding described is that KAI-9803 was rapidly delivered throughout the body to many tissues including the primary target organ, the heart, and most importantly, that KAI-9803 was effectively delivered into a variety of cells including cardiac myocytes and cardiac endothelial cells by a TAT_{47-57} mediated process.

Whole-body autoradioluminograms (Fig. 5) and microscopic observation (Fig. 6) showed that intravenously delivered KAI-9803 was distributed at high levels to the liver, kidneys, lungs and heart, and that KAI-9803 was taken up into the specific cells within these organs. These results support previous findings that intraperitoneal injection of 0.2 mg/kg of KAI-9803 resulted in significant inhibition of δPKC translocation in those organs (Begley et al., 2004), suggesting that those tissues were sufficiently exposed to KAI-9803 after intravenous injection to demonstrate a measurable pharmacodynamic effect. Previous findings in a pig model of acute myocardial infarction demonstrated that endothelial cells and cardiomyocytes were the target cells for cardioprotection of KAI-9803 from ischemia/reperfusion damage (Inagaki et al., 2003b). The microscopic observation (Fig. 6) clearly showed that KAI-9803 effectively entered these target cells

DMD Fast Forward. Published on June 28, 2011 as DOI: 10.1124/dmd.111.040725
This article has not been copyedited and formatted. The final version may differ from this version.

when delivered intravenously.

Some reports have shown that TAT_{47-57}-conjugated small peptides and macromolecules can be distributed to the brain through the blood-brain barrier after dosing *in vivo* (Aarts et al., 2002; Schwarze et al., 1999). In support of this conclusion, it was shown that a single intraperitoneal delivery of KAI-9803 at a dose of 0.2 mg/kg reduced damage to the microvascular endothelial cells and cerebral tissue, and decreased the infarct size in a rat model of cerebral ischemia (Bright et al., 2007). KAI-9803 was found to be delivered into the parenchyma through the blood-brain barrier when administered by an internal carotid arterial injection (Bright et al., 2004). In the present study, the macroscopic (Fig. 5) and microscopic observations (Fig. 6) showed that KAI-9803 was seen only in the cerebral blood vessels but not in the brain parenchyma 1 minute after being administered by an intravenous bolus. This result is similar to results seen by Xia and colleagues (Xia et al., 2001), using TAT_{47-57}-conjugated β-galactosidase administered intraperitoneally. The difference in brain distribution of KAI-9803 between the present study and prior publications may be the result of different sampling times and delivery routes. In the present study it appears that a one minute exposure is not sufficient to allow penetration of KAI-9803 through the blood-brain barrier, suggesting that another delivery approach, such as intravenous infusion, may be a more appropriate way of effectively delivering this compound to the brain.

The conjugation of TAT_{47-57} to proteins such as β-galactosidase facilitates their delivery throughout the body after intraperitoneal injection (Schwarze et al., 1999; Xia et al., 2001; Cai et al., 2006). In the present study, we examined the TAT_{47-57}-mediated tissue uptake of the peptide, KAI-9803, by comparing the tissue distribution of

DMD Fast Forward. Published on June 28, 2011 as DOI: 10.1124/dmd.111.040725
This article has not been copyedited and formatted. The final version may differ from this version.

^{125}I-labeled KAI-9803 to that of ^{125}I-labeled cargo peptide alone (Fig. 7). Levels of intact KAI-9803 were significantly higher in the heart, kidney, liver and in the spleen compared with levels of the cargo alone. These results reinforce that the TAT_{47-57} peptide facilitates the distribution of KAI-9803 to the tissues such as liver, kidneys and heart, as well as allowing penetration into the cells as previously reported (Chen et al., 2001b). The dependence of the CPP, TAT_{47-57}, on cellular uptake was further demonstrated by the results of the *in vivo* study with high doses of heparin. In these experiments, pre-treating the rats with very high doses of negatively charged heparin was able to reduce uptake of KAI-9803 into a number of tissues, presumably by competing with the cell surface proteoglycans for TAT-binding. However, clinically relevant doses of heparin (i.e., 1 mg/kg) did not interfere with the ability of KAI-9803 to distribute to tissues.

In contrast to what was seen in the other organs, in the lung the distribution of the cargo peptide and KAI-9803 were equivalent. It is possible that the association of the unconjugated cargo peptide is driven by non-specific, lipophilic interactions in this organ, as the cargo peptide is more lipophilic than KAI-9803. This result highlights the limitations of relying purely on such a non-specific, macroscopic assay for tissue distribution. Cellular uptake was examined in more detail by using an *in vitro* cell culture system of primary rat cardiomyocytes. In these experiments (Fig. 8), it was clearly demonstrated that ^{125}I-KAI-9803 is quickly taken up into a relevant cell type, in a process dependent upon the presence of the TAT CPP.

^{14}C-KAI-9803 was shown to be rapidly degraded and cleared from the systemic circulation within five minutes after an intravenous injection to rats (Fig. 3). Because there are high protease concentrations in the circulation, KAI-9803 is most likely

DMD Fast Forward. Published on June 28, 2011 as DOI: 10.1124/dmd.111.040725
This article has not been copyedited and formatted. The final version may differ from this version.

cleared by proteolytic degradation. In a preliminary *in vitro* study, KAI-9803 was unstable in rat plasma with a half-life of approximately 5 minutes at 37C˚ (data not shown). However, the present study demonstrated that the elimination from the circulation was even faster, with a half-life of less than two minutes. We believe that the majority of KAI-9803 is cleared rapidly from the circulation by uptake into tissues and that the portion of KAI-9803 which is not delivered to tissues is quickly degraded. Given the strong interaction between TAT_{47-57} and the proteoglycans on the cell surface, it is likely that tissue uptake is responsible for the majority of the apparent rapid clearance of KAI-9803 from the systemic circulation. In fact, when the tissue distribution of ^{125}I-KAI-9803 was inhibited by a high dose of heparin, the blood level of ^{125}I-KAI-9803 increased to about double that of the control group (Fig. 7). The increased circulating blood concentrations may account for the increased renal exposure of ^{125}I-KAI-9803 in the presence of high doses of heparin, given the role of the kidneys in clearing low molecular weight peptides from the systemic circulation. It is possible that KAI-9803 may be more efficiently delivered to human tissues than to rat tissues, because KAI-9803 was more stable in human plasma *in vitro* with the half-life of 80 minutes (data not shown).

In conclusion, the present study demonstrated that KAI-9803 was effectively delivered into the target cells such as cardiac myocytes and cardiac endothelial cells within 1 minute after a single intravenous administration. The distribution of KAI-9803 to tissues such as the liver, kidney heart and spleen was facilitated by the reversible conjugation to TAT_{47-57}. The intracellular delivery of the cargo peptide into the cardiomyocytes was mediated by the TAT_{47-57} carrier peptide. These data support previous preclinical and clinical findings of efficacy suggesting an intravenous drug of

KAI-9803 could have potential for the treatment of ischemia/reperfusion injury.

DMD Fast Forward. Published on June 28, 2011 as DOI: 10.1124/dmd.111.040725
This article has not been copyedited and formatted. The final version may differ from this version.

Acknowledgements

We gratefully acknowledge Dr. Kenichi Sudo for the helpful and insightful discussion.

Authorship Contributions

Participated in research design: Miyaji, Walter, Chen, and Okazaki.

Conducted experiments: Miyaji, Ishizuka, Saito, and Kawai.

Contributed new reagents or analytic tools: Walter, and Chen

Performed data analysis: Miyaji and Kurihara.

Wrote or contributed to the writing of the manuscript: Miyaji, Walter, Kurihara, Okazaki.

References

Aarts M, Liu Y, Liu L, Besshoh S, Arundine M, Gurd JW, Wang YT, Salter MW, and Tymianski M. (2002) Treatment of ischemic brain damage by perturbing NMDA receptor- PSD-95 protein interactions. *Science* **298:** 846-850.

Bates E, Bode C, Costa M, Gibson CM, Granger C, Green C, Grimes K, Harrington R, Huber K, Kleiman N, Mochly-Rosen D, Roe M, Sadowski Z, Solomon S, and Widimsky P (2008) Intracoronary KAI-9803 as a Adjunct to Primary Percutaneous Coronary Intervention for Acute ST-Segment Elevation Myocardial Infarction. *Circulation* **117:** 886-896.

Begley R, Liron T, Baryza J, and Mochly-Rosen D (2004) Biodistribution of intracellularly acting peptides conjugated reversibly to Tat. *Biochem Biophys Res Commun* **318:** 949-954.

Bright R, Raval AP, Dembner JM, Perez-Pinzon MA, Steinberg GK, Yenari MA, and Mochly-Rosen D (2004) Protein kinase C delta mediates cerebral reperfusion injury *in vivo*. *J Neurosci* **24:** 6880-6888.

Bright R, Steinberg GK, Mochly-Rosen D (2007) DeltaPKC mediates microcerebrovascular dysfunction in acute ischemia and in chronic hypertensive stress *in vivo. Brain Res* **1144:** 146-155.

Cai SR, Xu G, Becker-Hapak M, Ma M, Dowdy SF, and McLeod HL (2006) The kinetics and tissue distribution of protein transduction in mice. *Eur J Pharm Sci* **27:** 311-319.

Chen L, Hahn H, Wu G, Chen CH, Liron T, Schechtman D, Cavallaro G, Banci L, Guo Y, Bolli R, Dorn GW and, Mochly-Rosen D (2001a) Opposing cardioprotective actions and parallel hypertrophic effects of delta PKC and epsilon PKC. *Proc Natl Acad Sci U S A* **98:** 11114-11119.

Chen L, Wright LR, Chen CH, Oliver SF, Wender PA and Mochly-Rosen D (2001b) Molecular transporters for peptides: delivery of a cardioprotective epsilonPKC agonist peptide into cells and intact ischemic heart using a transport system, R(7). *Chem Biol* **8:** 1123-1129.

Console S, Marty C, Garcia-Echeverria C, Schwendener R, and Ballmer-Hofer K. (2003) Antennapedia and HIV transactivator of transcription (TAT) "protein transduction domains" promote endocytosis of high molecular weight cargo upon binding to cell surface glycosaminoglycans. *J Biol Chem* **278:** 35109-35114.

Harada H, Hiraoka M, Kizaka-Kondoh S. (2002) Antitumor effect of TAT-oxygen-dependent degradation-caspase-3 fusion protein specifically stabilized and activated in hypoxic tumor cells. *Cancer Res*. **62:** 2013-2018.

Ikeno F, Inagaki K, Rezaee M, and Mochly-Rosen D (2007) Impaired perfusion after

myocardial infarction is due to reperfusion-induced deltaPKC-mediated myocardial damage. *Cardiovasc Res* **73:** 699-709.

Inagaki K, Chen L, Ikeno F, Lee FH, Imahashi K, Bouley DM, Rezaee M, Yock PG, Murphy E, and Mochly-Rosen D (2003a) Inhibition of delta-protein kinase C protects against reperfusion injury of the ischemic heart *in vivo*. *Circulation* **108:** 2304-2307.

Inagaki K, Hahn HS, Dorn GW 2nd, Mochly-Rosen D (2003b) Additive protection of the ischemic heart ex vivo by combined treatment with delta-protein kinase C inhibitor and epsilon-protein kinase C activator. *Circulation* **108:** 869-875.

Kaplan IM, Wadia JS, and Dowdy SF (2005) Cationic TAT peptide transduction domain enters cells by macropinocytosis. *J Controlled Release* **102:** 247-253

Mochly-Rosen D (1995) Localization of protein kinases by anchoring proteins: a theme in signal transduction. *Science* **268:** 247-251.

Mochly-Rosen D, and Gordan AS (1998) Anchoring proteins for protein kinase C: a means for isozyme selectivity. *FASEB J* **12:** 35-42.

Schwarze SR, Ho A, Vocero-Akbani A, and Dowdy SF (1999) *In vivo* protein transduction: delivery of a biologically active protein into the mouse. *Science* **285:** 1569-72.

Thorell JI, and Johansson BG (1971) Enzymatic iodination of polypeptides with ^{125}I to high specific activity. *Biochim Biophys Acta* **251:** 363-369.

Tünnemann G, Martin RM, Haupt S, Patsch C, Edenhofer F, Cardoso MC. (2006) Cargo-dependent mode of uptake and bioavailability of TAT-containing proteins and peptides in living cells. *FASEB J.* **20:** 1775-1784.

Tyagi M, Rusnati M, Presta M, and Giacca M (2001) Internalization of HIV-1 tat requires cell surface heparan sulfate proteoglycans. J Biol Chem **276:** 3254-3261.

Xia H, Mao Q, and Davidson BL (2001) The HIV Tat protein transduction domain improves the biodistribution of beta-glucuronidase expressed from recombinant viral vectors. *Nat Biotechnol* **19:** 640-644.

Yuki K, Miyauchi T, Kakinuma Y, Murakoshi N, Suzuki T, Hayashi J, Goto K, and Yamaguchi I (2000) Mitochondrial dysfunction increases expression of endothelin-1 and induces apoptosis through caspase-3 activation in rat cardiomyocytes in vitro. *J Cardiovasc Pharmacol* **36:** S205-S208.

DMD Fast Forward. Published on June 28, 2011 as DOI: 10.1124/dmd.111.040725
This article has not been copyedited and formatted. The final version may differ from this version.

Footnotes

Address correspondence to:

Yoshihiro Miyaji

Drug Metabolism and Pharmacokinetics Research Laboratories, Daiichi Sankyo Co., Ltd., 1-2-58, Hiromachi, Shinagawa-ku, Tokyo 140-8710, Japan.

Tel: +81-3-3492-3131

Fax: +81-3-5436-8567

E-mail: miyaji.yoshihiro.kc@daiichisankyo.co.jp

Figure Legends

Fig. 1 Chemical structure of KAI-9803 (A) and cargo petpide (B). *, marks the position of the ^{14}C-label.

Fig. 2 The profile of blood (open circle) and plasma (closed circle) concentrations of radioactivity versus time after intravenous administration of ^{14}C-KAI-9803 at a dose of 1 mg/kg to rats. Data are the mean ± S.D. from three rats.

Fig. 3 Typical HPLC chromatograms of ^{14}C-labeled KAI-9803 in the dosing solution and plasma (A) and the remaining ratio of unchanged ^{14}C-KAI-9803 in plasma determined by RP-HPLC (B). Plasma samples were collected at 1, 2 and 5 minutes after intravenous administration of ^{14}C-KAI-9803 at a dose of 10 mg/kg to rats. RP-HPLC chromatogram at 1 and 5 minutes are shown. Data are the mean ± S.D. from three rats.

Fig. 4 Cumulative biliary and urinary excretion ratio of radioactivity (% of dose) after intravenous administration of ^{14}C-KAI-9803. Open triangle and closed triangle show the cumulative ratio for bile and urine, respectively. A closed circle shows the sum of the biliary and urinary excretion ratios. Data are the mean ± S.D. from four rats.

Fig. 5 Whole-body tissue distribution of ^{14}C-KAI-9803 at 1 minute after intravenous administration of ^{14}C-KAI-9803 at a dose of 1 mg/kg to a rat. (A) Whole body autoradioluminograms. (B) Calculated microgram-equivalents of ^{14}C-KAI-9803.

Fig. 6 Microscopic autoradiograms of rat tissues at 1 minute after intravenous administration of ^{14}C-KAI-9803. Distribution of radioactivity was confirmed by black grain (bright field, upper panel) and white grain (dark field, lower panel) in the hematoxylin and eosin-stained section. (Scale bars represent 92.5 μm in A and B, and 100 μm in C, D, E, F, G and H). (A) Bright field and (B) dark field of the liver, the blood vessels (BV), the bile duct (BD). (C) Bright field and (D) dark field of the kidney; the glomeruli (GI). (E) Bright field and (F) dark field of the lungs; the smooth muscle (SM), the bronchioles (Br). (G) Bright field and (H) dark field of the heart; the cardiac myocytes (My), the blood vessels (BV). (I) Bright field and (J) dark field of the brain; the blood vessel (BV), the caudate putamen (CPu) located 0.48 mm anterior from Bregma.

Fig. 7 Tissue distribution of ^{125}I-KAI-9803 and ^{125}I-cargo peptide after intravenous administration to rats. Each administration of ^{125}I-KAI-9803 (open bar) and ^{125}I-cargo peptide (solid bar) was injected at a dose of 0.35 μmol/kg at 1 minute after the administration of 4% mannitol solution. Heparin was injected at doses of 1 mg/kg (shaded bar) or 100 mg/kg (gray bar) 1 minute before the dosing of ^{125}I-KAI-9803. Data are the mean ± S.D. from at least four rats. Significant differences from the control were determined by Dunnett's test (*; $p< 0.05$, **; $p< 0.01$, ***; $p< 0.001$).

Fig. 8 Time-course of the internalization of ^{125}I-KAI-9803 and ^{125}I-cargo peptide to rat

DMD Fast Forward. Published on June 28, 2011 as DOI: 10.1124/dmd.111.040725
This article has not been copyedited and formatted. The final version may differ from this version.

cardiomyocytes. The cells were incubated with 10 nM of ^{125}I-KAI-9803 at 37˚C (closed circle) and at 4˚C (closed triangle), and ^{125}I-cargo peptide at 37˚C (open circle). Data are the mean ± S.E. from three experiments.

Fig. 1

(A) KAI-9803

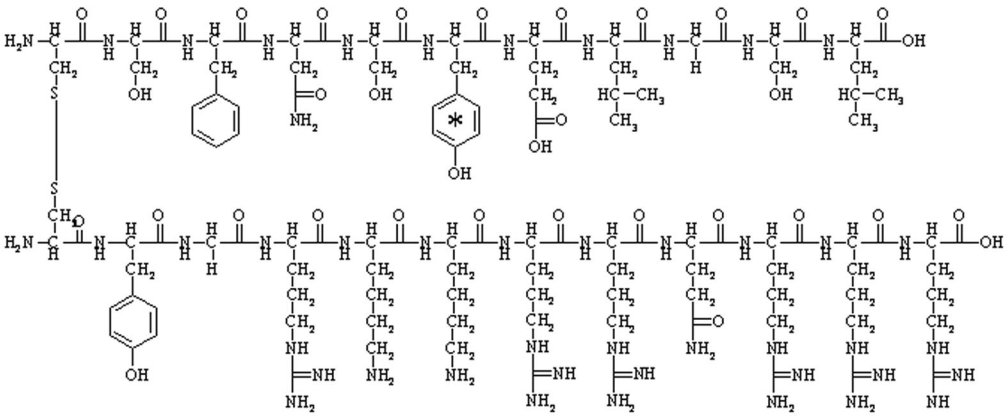

(B) δV1-1

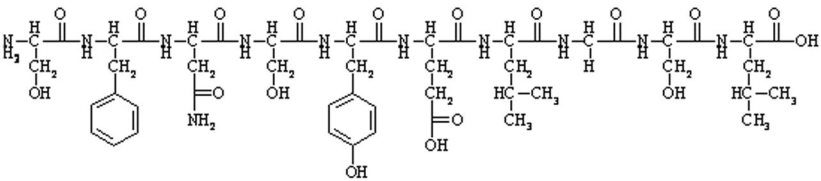

Fig. 2

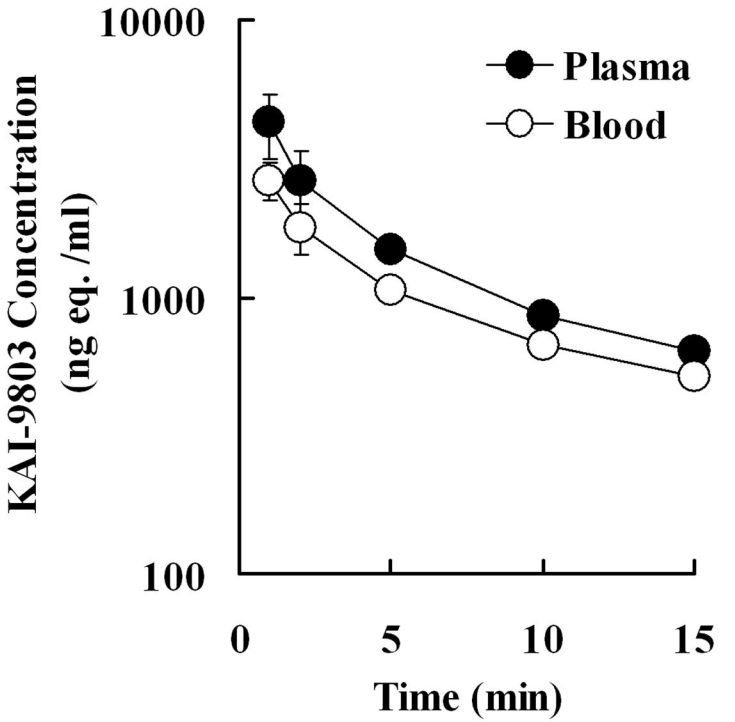
10000
1000
100
KAI-9803 Concentration
(ng eq. /ml)
Plasma
Blood
0
5
10
15
Time (min)

Fig. 3

(A)

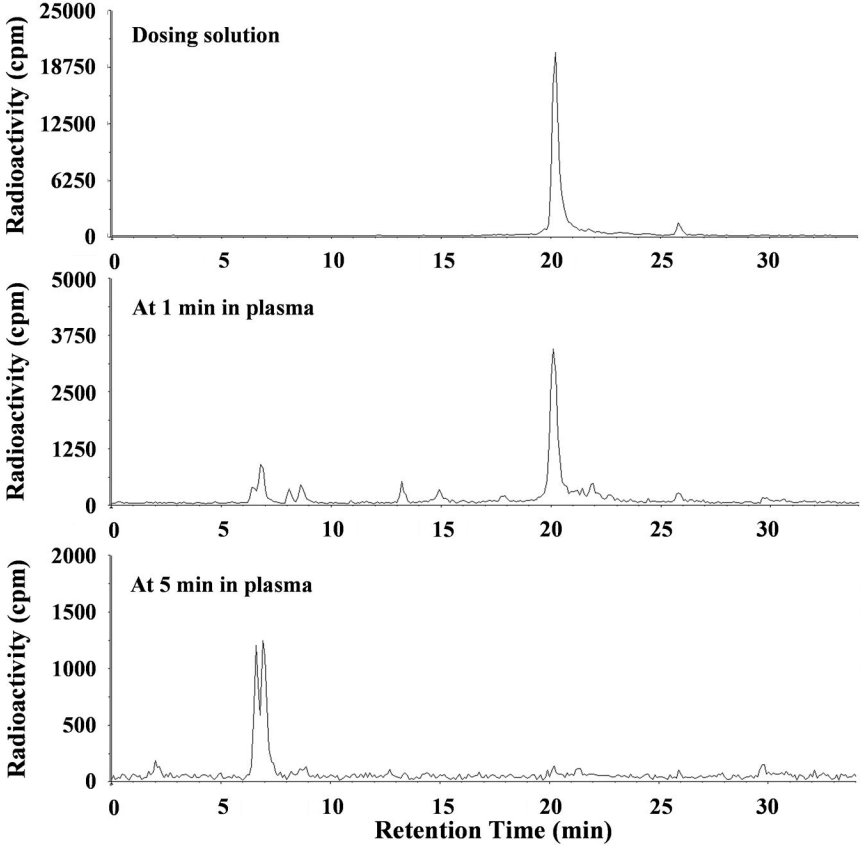
Dosing solution
At 1 min in plasma
At 5 min in plasma
Radioactivity (cpm)
25000
18750
12500
6250
0
5000
3750
2500
1250
2000
1500
1000
500
0
5
10
15
20
25
30
Retention Time (min)

(B)

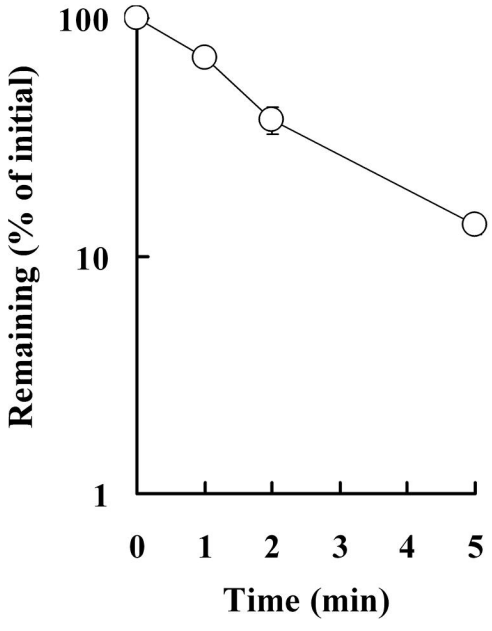
Remaining (% of initial)
100
10
1
0
1
2
3
4
5
Time (min)

Fig. 4

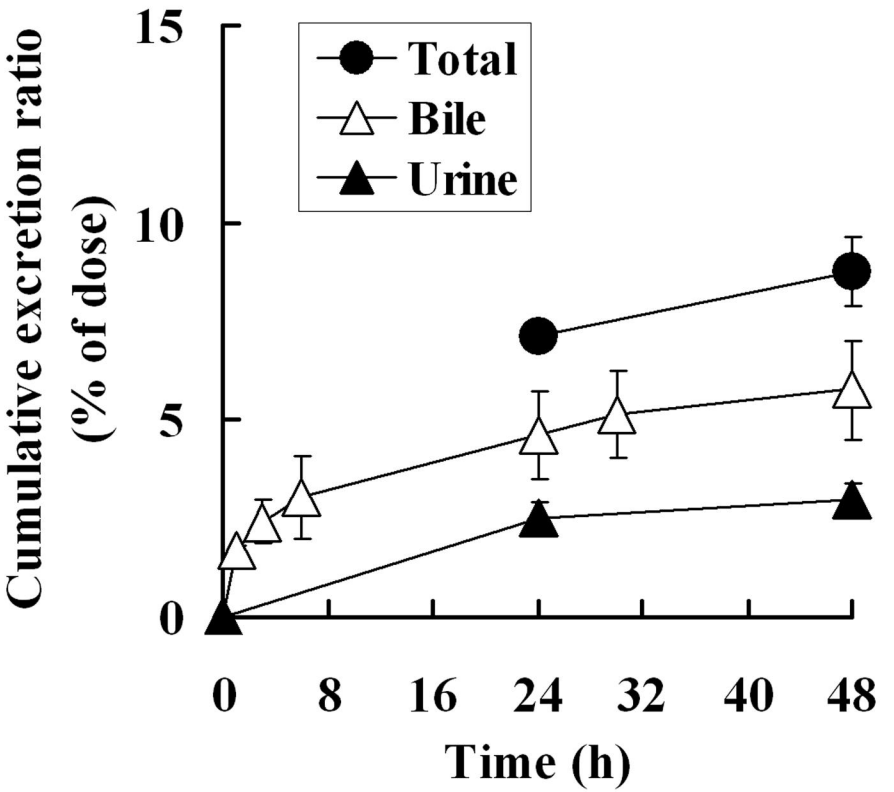
Cumulative excretion ratio
(% of dose)
15
10
5
0
Total
Bile
Urine
0
8
16
24
32
40
48
Time (h)

Fig. 5

(A)

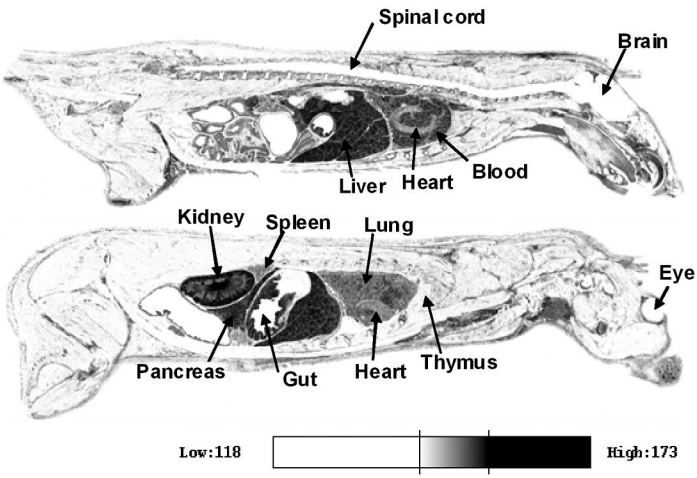
Spinal cord
Brain
Liver
Heart
Blood
Kidney
Spleen
Lung
Eye
Pancreas
Gut
Heart
Thymus
Low:118
High:173

(B)

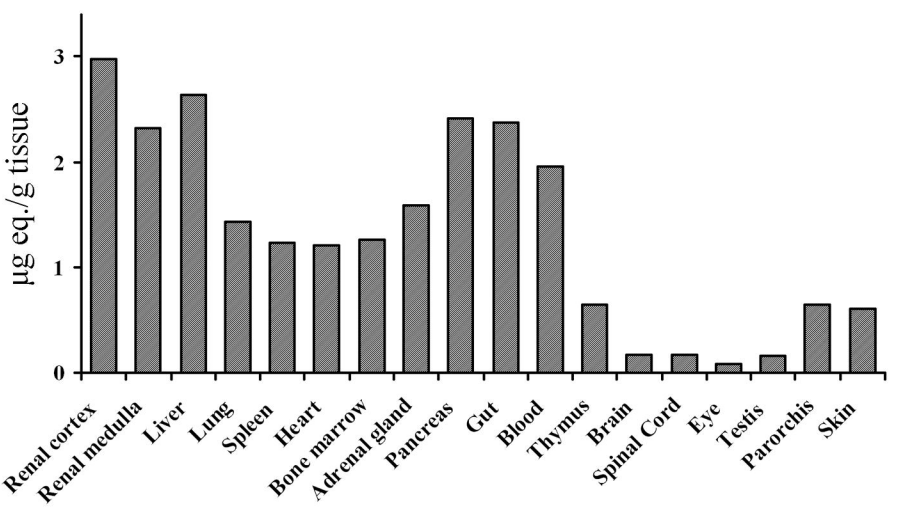
μg eq./g tissue
0
1
2
3
Renal cortex
Renal medulla
Liver
Lung
Spleen
Heart
Bone marrow
Adrenal gland
Pancreas
Gut
Blood
Thymus
Brain
Spinal Cord
Eye
Testis
Parorchis
Skin

Fig. 6

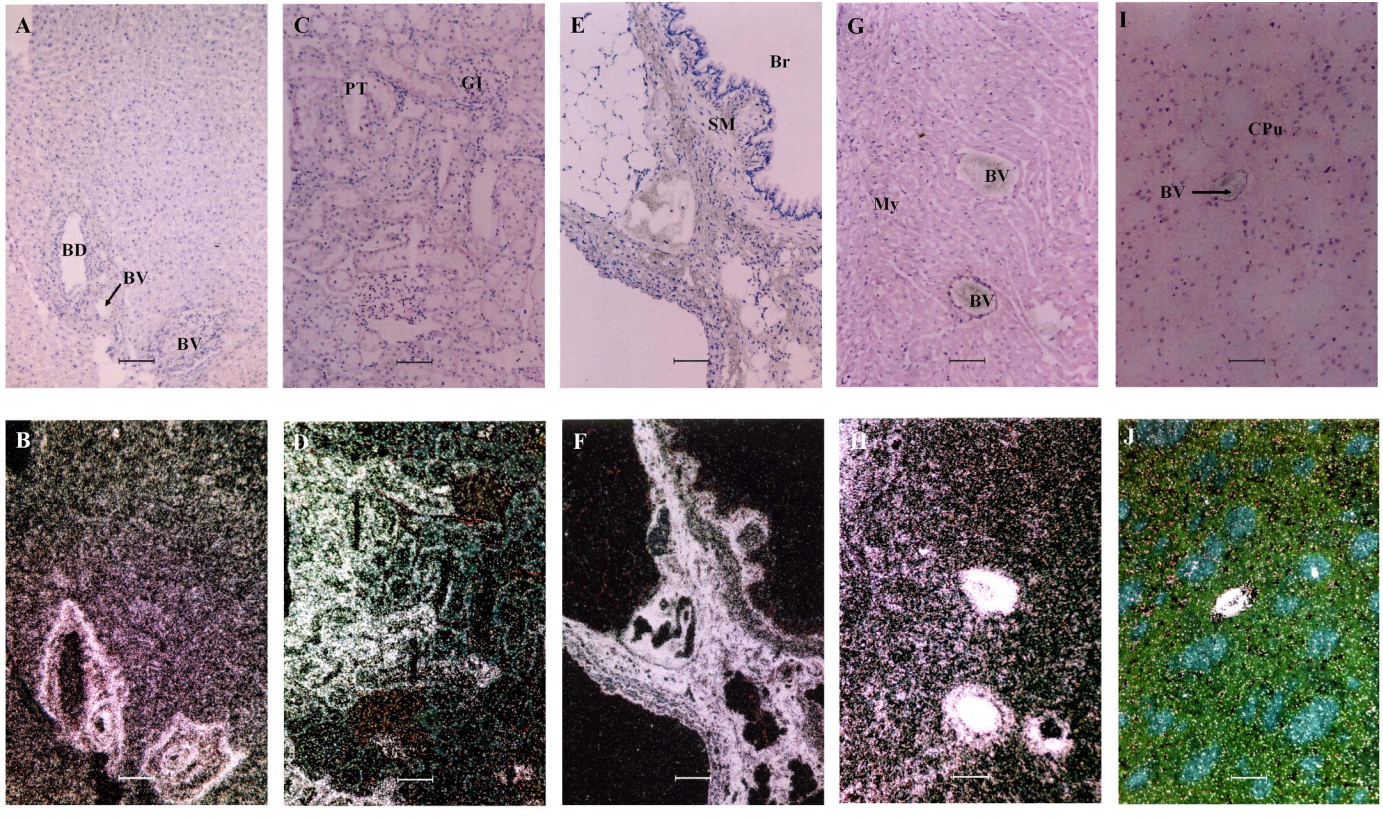

Fig. 7

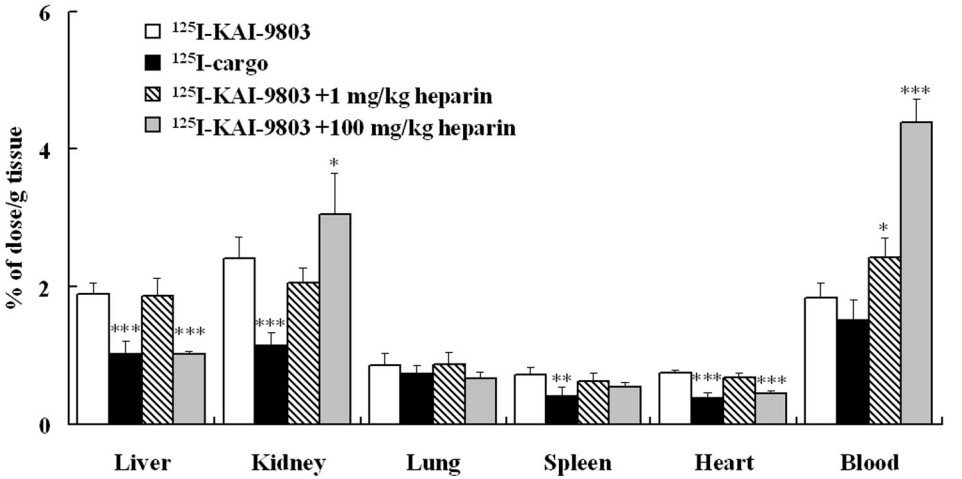
6
4
2
0
% of dose/g tissue
125I-KAI-9803
125I-cargo
125I-KAI-9803 +1 mg/kg heparin
125I-KAI-9803 +100 mg/kg heparin
***
***
***
*
***
**
***
***
*
***
Liver
Kidney
Lung
Spleen
Heart
Blood

Fig. 8

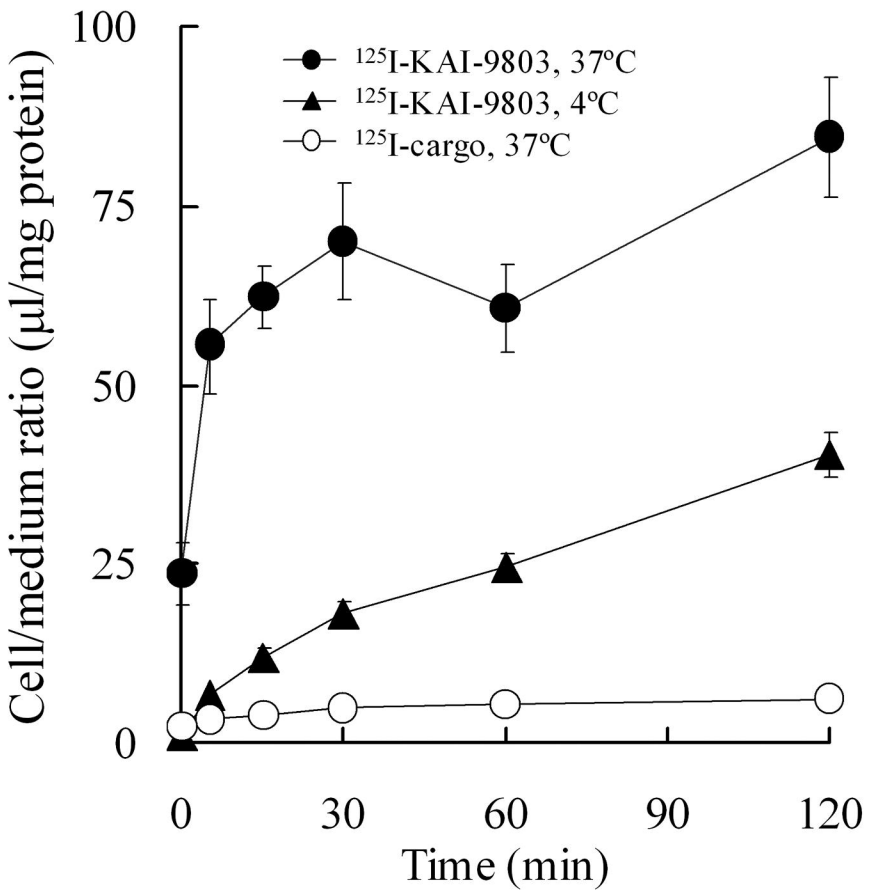
100
75
50
25
0
Cell/medium ratio (μl/mg protein)
125I-KAI-9803, 37ºC
125I-KAI-9803, 4ºC
125I-cargo, 37ºC
0
30
60
90
120
Time (min)